

### 3.1 Efficient Power Management Circuit: Thermal Energy Harvesting to Above-IC Microbattery Energy Storage

H. Lhermet<sup>1</sup>, C. Condemine<sup>1</sup>, M. Plissonnier<sup>2</sup>, R. Salot<sup>2</sup>,  
P. Audebert<sup>1</sup>, M. Rosset<sup>1</sup>

<sup>1</sup>CEA/LETI, Grenoble, France

<sup>2</sup>CEA/LITEN, Grenoble, France

Autonomous devices that are self-powered over a full lifetime, by extracting their energy from the environment, are crucial for applications such as ambient intelligence, active security in smart cards or monitoring. As the energy availability and power dissipation are not constant over time, energy management becomes a key function and determines the potential for information processing. All these challenging constraints have been taken into account to develop an autonomous system enabling thermal energy harvesting and power storage in the microwatt range.

The microsystem architecture, illustrated in Fig. 3.1.1, is comprised of two power sources, RF and thermoelectric, a microbattery used as a storage unit and integrated circuits to transform and manage the harvested energy and interface the microbattery. Both sources are managed by the ICs: the microbattery being charged either using thermal energy harvested by the thermogenerator associated with the DC/DC converter or using external RF power converted by the RF converter. The state of charge of the storage device is monitored periodically.

Thermoelectric power generators have three main advantages: no human intervention is required throughout their lifetime, they are highly reliable and quiet since there are no moving mechanical parts and the materials used are environment friendly. Micro and nanotechnologies enable production of the small power generators required to match the decreasing dimensions of standard wireless sensor modules. The thermal micro-generator illustrated in Fig. 3.1.2 has an output power of  $4\mu\text{W}/\text{cm}^2$  per degree C, a  $90\Omega$  series resistance and generates 1V for a temperature difference of  $60^\circ\text{C}$ .

A micropower up-converter switching power supply is used to convert the available power from the thermogenerator into a regulated power supply (Fig. 3.1.3). The difference between one part of the boost filter output voltage ( $\alpha \cdot V_{\text{out}}$ ) and a voltage setpoint (SP) is amplified, then modulated into pulse density information for control of the MOS power switch. A sub-1V bandgap voltage reference [1] is used as the voltage reference (570mV). The error amplifier is comprised of a 50dB gain OTA and a buffer. The innovative pulse density modulation (PDM) is based on an asynchronous passive  $\Delta\Sigma$  modulator instead of the traditional PWM controller for simplicity of implementation (2 RC filters and 3 inverters), very low power consumption ( $1\mu\text{W}$ ) and spectral spread of the switch noise. A low-voltage, high-performance charge pump, composed of one clock booster and two stages of voltage doublers [2], is used to increase the PDM signal voltage four-fold. This allows a large decrease in the equivalent Ron of the MOS switch.

The RF converter is composed of a limiter, a rectifier and a control loop to provide a stabilised DC output. In standard 13.56MHz RFID applications, RF power and conversion efficiency depend on the distance between the RF source and the IC; the input RF power is much greater than the needed power and the superfluous current is diverted through ballast MOS.

The microbattery can be charged by the thermogenerator's DC/DC output or by the RF converter. Therefore, the power supply manager, comprising a specific unit along with an asynchronous finite state machine, manages priority between the two sources when they are present simultaneously and activates self-

powered microbattery protection in the case of external power source interruption. The charge controller provides constant current for a one hour microbattery charge.

The lithium, solid-state microbatteries [3] are processed on Si wafers using thin film technology. The low process temperature ( $< 350^\circ\text{C}$ ) required and surface compatibility with ASIC materials allow the use of the ASIC as a substrate for the microbattery.

In order to ensure permanent monitoring, the microbattery discharge monitor is supplied by the above-IC deposited microbattery itself. Therefore, since the available capacity provided by these on-chip batteries is in the range of  $100\mu\text{Ah}/\text{cm}^2$ , all levels of monitor development (from architecture to design) are made to achieve an ultra-low-power monitor [4, 5], the aim being longer battery operation and preservation of energy for the application. The discharge monitor must also be resistant to supply voltage variations (1.6V to 2.8V) to be compatible with the microbattery. The microbattery is considered discharged if its voltage is lower than  $1.6\text{V} \pm 0.1\text{V}$ . The discharge monitor compares this voltage to a reference voltage for one second every hour. This sampling rate is sufficient since the microbattery lasts for about one year for the envisaged low duty-cycle applications.

The DC/DC converter for the thermogenerator illustrated in Fig. 3.1.4 is implemented in a traditional  $0.35\mu\text{m}$  CMOS process and occupies a core area of  $0.5\text{mm}^2$ . Measurement results indicate a total power consumption of  $70\mu\text{W}$  with a 1V supply voltage, including clock generation, charge pump,  $\Delta\Sigma$  modulator, error amplifier, bandgap reference and I/O pads (Fig. 3.1.5). The bandgap reference presents a voltage variation of  $104\text{ppm}/^\circ\text{C}$  in a  $[-40, +160]^\circ\text{C}$  temperature range. The output voltage can be regulated within a 2.5V range from 1.75V to 4.3V. Figure 3.1.6 shows DC/DC converter block efficiency at maximum output current for different voltage levels. Higher efficiency is obtained for a 1.75V output and maximum output power is obtained at an output voltage of 2.25V. The efficiency factor can be strongly enhanced by reducing losses in the power filter (and especially in the diode).

Figure 3.1.7 illustrates an IC, containing an RF converter, the power supply manager and the microbattery charger and discharge monitor, fabricated in  $0.18\mu\text{m}$  CMOS with a  $30\text{mm}^2$  microbattery deposited on the surface. A 78% efficient power supply management and microbattery charge unit is obtained with a  $27\mu\text{A}$  charge current and a 12pA standby current consumption from the microbattery (for permanently supplied protection). The overall consumption of the battery-powered discharge monitor is less than  $5\text{nW}$  ( $3.3\text{nW}$  for sequencing,  $1.3\text{nW}$  for sampled comparison, as detailed in Fig. 3.1.5). These results are confirmed by system level tests with above-IC microbattery powered ASICs, showing furthermore that the microbattery process does not affect ASIC performance.

In order to achieve thermal energy harvesting and storage, a micropower DC/DC up-converter and a controller chipset was designed and tested. The next step of this project is to design an autonomous microsystem including the two proposed functions together with a traceability application in the same die and technology.

#### References:

- [1] K. Lasanen, V. Korkala, E. Raisanen-Ruotsalainen, J. Kostamovaara, "Design of a 1-V Low Power CMOS Bandgap Reference Based on Resistive Subdivision", *IEEE MWSCAS*, vol. 3, pp. 564-567, Aug., 2002.
- [2] Y. Moisiadis, I. Bouras, A. Arapoyanni, "Charge Pump Circuits for Low-Voltage Applications," *VLSI Design*, vol.15, pp. 477-483, Jan., 2002.
- [3] C. Navone, R. Baddour-Hadjean, J. P. Pereira-Ramos, and R. Salot "High-Performance Oriented V2O5 Thin Films Prepared by DC Sputtering for Rechargeable Lithium Microbatteries," *J. Electrochem. Soc.*, vol. 152(9), p. A1790-1796, 2005.
- [4] H.J. Oguey, and D. Aebischer, "CMOS Current Reference Without Resistance," *IEEE J. Solid-State Circuits*, vol. 32, pp. 1132-1135, July 1997.
- [5] S.F. Al-Sarawi, "Low Power Schmitt Trigger Circuit," *Electronics Letters*, vol. 38, no.18, pp. 1009-1010, Aug. 29, 2002.

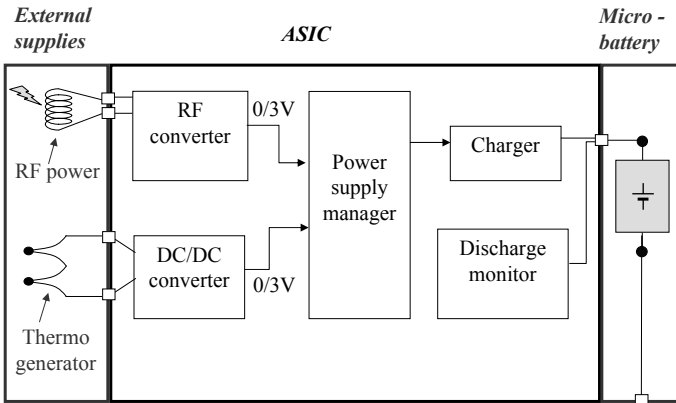


Figure 3.1.1: System architecture.

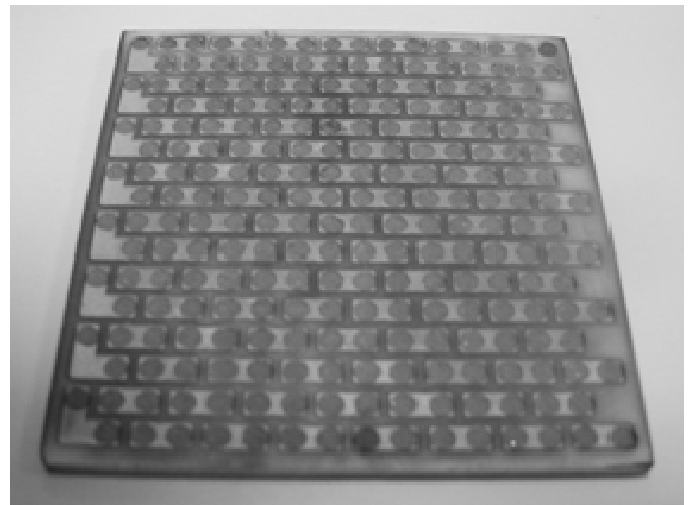


Figure 3.1.2: Thermo-elements.

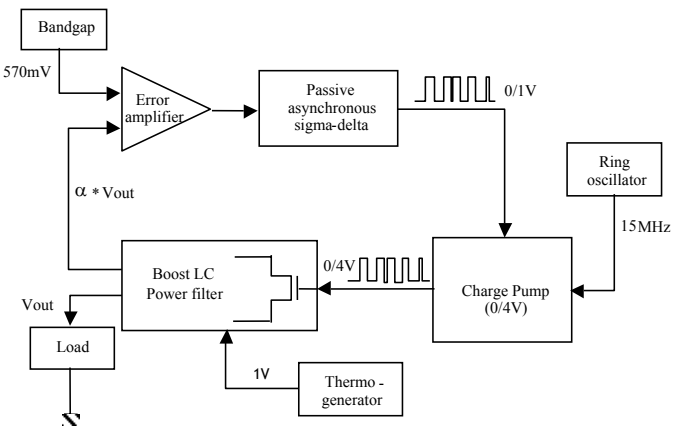


Figure 3.1.3: DC/DC converter architecture.

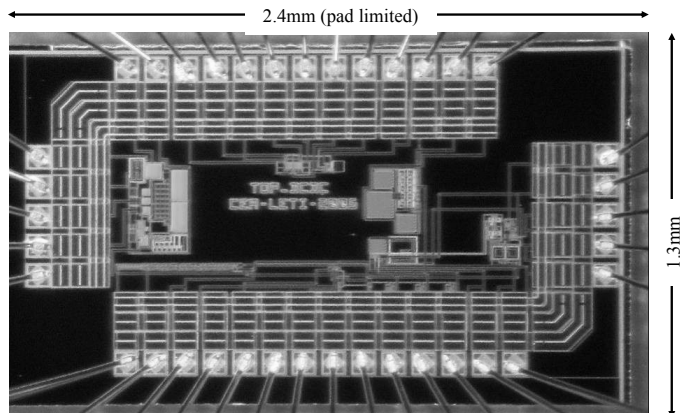


Figure 3.1.4: Thermal DC/DC converter micrograph.

	Simulation	Test
<b>DC/DC converter</b>	<b>46µA</b>	<b>70µA</b>
Bandgap reference	6.1µA	7µA
Error amplifier	5µA	5µA
Asynchronous passive ΔΣ	1.1µA	1.1µA
Clock generator and IO pads	10.8µA	26.9µA
Charge pump and MOS power switch	23µA	30µA
<b>Microbattery discharge monitor</b>	<b>2.2nA</b>	<b>2.17nA</b>
Sequencing signal generation	1.60nA	1.52nA
Current reference	1.05nA	
Oscillator	450pA	400pA
Schmitt trigger	40pA	<10pA
Frequency 2 <sup>12</sup> divider	40pA	10pA
Sequencing signal shaping	20pA	50pA
<b>Sampled comparison (bandgap, adaptation and comparator)</b>	<b>605pA</b>	<b>596pA</b>
Active current consumption (act time = act period/2 <sup>12</sup> )	2.2µA	1.87µA
Standby current consumption	68pA	140pA
<b>Hold</b>	<b>60pA</b>	<b>&lt;10pA</b>

Figure 3.1.5: Current consumption.

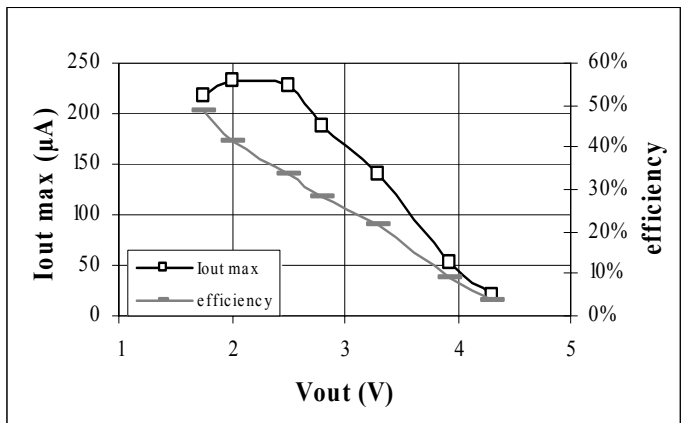


Figure 3.1.6: DC/DC converter efficiency.

Continued on Page 587

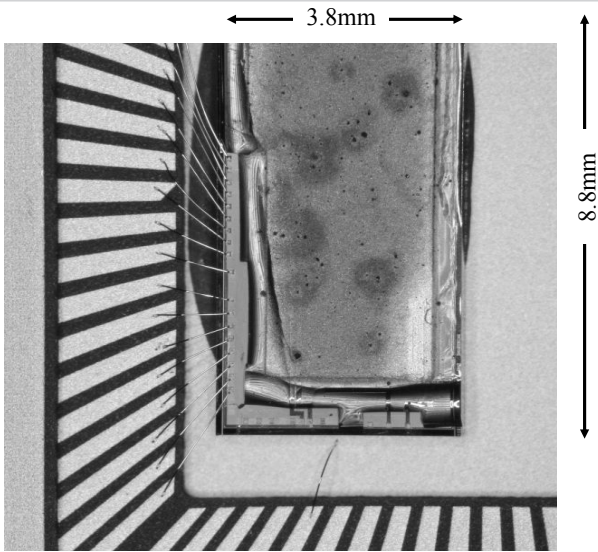


Figure 3.1.7: Discharge monitoring die with above-IC microbattery.